Degenerate fermion dark matter from a broken $U(1)_{B\text{-}L}$ gauge symmetry

Gongjun Choi,[1,*] Motoo Suzuki,[1,†] and Tsutomu T. Yanagida[1,2,‡]

[1]*Tsung-Dao Lee Institute, Shanghai Jiao Tong University, Shanghai 200240, China*
[2]*Kavli IPMU (WPI), UTIAS, The University of Tokyo, 5-1-5 Kashiwanoha, Kashiwa, Chiba 277-8583, Japan*

(Received 27 April 2020; accepted 17 July 2020; published 21 August 2020)

The extension of the Standard Model by assuming $U(1)_{B\text{-}L}$ gauge symmetry is very well motivated since it naturally explains the presence of heavy right-handed neutrinos required to account for the small active neutrino masses via the seesaw mechanism and thermal leptogenesis. Traditionally, we introduce three right-handed neutrinos to cancel the $[U(1)_{B\text{-}L}]^3$ anomaly. However, it suffices to introduce two heavy right-handed neutrinos for these purposes and therefore we can replace one right-handed neutrino by new chiral fermions to cancel the $U(1)_{B\text{-}L}$ gauge anomaly. Then, one of the chiral fermions can naturally play a role of a dark matter candidate. In this paper, we demonstrate how this framework produces a dark matter candidate which can address the so-called "core-cusp problem". As one of the small-scale problems that the Λ cold dark matter paradigm encounters, it may imply an important clue for the nature of dark matter. One of resolutions among many is hypothesizing that sub-keV fermion dark matter halos in dwarf spheroidal galaxies are in a (quasi) degenerate configuration. We show how the degenerate sub-keV fermion dark matter candidate can be nonthermally originated in our model and thus can be consistent with the Lyman-α forest observation. Thereby, the small neutrino mass, baryon asymmetry, and the sub-keV dark matter become consequences of the broken B-L gauge symmetry.

DOI: 10.1103/PhysRevD.102.035022

I. INTRODUCTION

Despite various evidences for the presence of dark matter (DM), DM's nature has not been uncovered yet. The central questions in regard to DM concerns a mass of DM, what nongravitational interaction DM does, and its stability. Answers to these questions are considered essential factors in understanding not only a history and structure of the Universe in cosmology, but also a bigger and more fundamental picture lying behind the Standard Model (SM) in particle physics. Seen from the perspective of this kind, DM related observational anomalies reported in the study of cosmology and astrophysics could serve as a critical hint for physics beyond the Standard Model (BSM) although it is not necessary.

With that being said, a well-known discrepancy between what has been expected based on a standard hypothesis of the cold dark matter (CDM) and what are observed regarding the small-scale structure (galactic or subgalactic scale) may deserve attention from a well-motivated BSM physics. Cuspy halo profiles of dwarf galaxies predicted by N-body simulations equipped with CDM [1–3] are at odds with the cored halo profiles implied by stellar kinematic data of low mass galaxies [4–8], which might be signaling a nature of DM deviating from collisionless and cold aspects. Along with "the missing satellite problem" [9,10] and the "too-big-to-fail problem" [11], this so-called "core-cusp problem" [12] is challenging for the most popular and robust CDM framework in spite of the success it has achieved thus far in accounting for the large scale structure of the Universe and evolution thereof.

Relying on predicted phenomenological consequences arising from a specific mass or nongravitational interaction that DM enjoys, several alternative frameworks to CDM have been suggested so far in an effort to address the core-cusp problem (and other small-scale issues as well). These include warm dark matter (WDM)[1]

*gongjun.choi@gmail.com
†m0t@icrr.u-tokyo.ac.jp
‡tsutomu.tyanagida@ipmu.jp

[1]Warm dark matter is assuming a DM particle characterized by a small enough mass to produce a free-streaming length of $\mathcal{O}(0.1)$ Mpc and also by nonzero velocity dispersion. This feature enables WDM to erase density perturbations for the scale smaller than its free-streaming length, and thereby suppression of the matter power spectrum on the small scale and of the formation of sub-halos is induced in comparison to the CDM case [13–18]. As for the core size of a dwarf galaxy, WDM N-body simulations were conducted to study how the primordial velocity dispersion of WDM affects the inner structure of DM halo in [19,20]. In particular, sub-keV WDM is shown to produce the halo core size of $\mathcal{O}(100)$ pc for a typical sub-halo mass of the Milky Way whereas WDM with 1–2 keV mass does the core of 10–50 pc [20].

[13,14,21], ultralight bosonic DM [22–24],[2] and self-interacting DM[3] [27].

Another interesting possibility of DM resulting in a cored halo profile in a low mass galaxy is the fermion DM in the quantum degenerate limit. Along the similar line, the hypothesis of the fermion DM as the self-gravitating (quasi) degenerate gas was invoked in [28–32] to explain the kinematics of dwarf spheroidal galaxies (dSphs). The fitting procedures for the kinematic data (stellar velocity dispersion and halo radius of dSphs) yielded a sub-keV mass regime as the possible fermion DM mass (see also Refs. [33–36] for more studies about sub-keV fermion DM). Because of this, sub-keV fermion DM can serve as a class of a solution to the core-cusp problem if it resides in dSphs nowadays with sufficiently low temperature so as to sit in the (quasi) degenerate state. This sub-keV mass regime encounters a severe constraint from the Lyman-α forest (see, e.g., [37–39]), but the solution can still be viable provided that the sub-keV fermion DM is nonthermally originated and the free-streaming length of DM is not too large to be consistent with constraints derived from the Lyman-α flux power spectrum. The free-streaming (FS) length range $0.3\ \mathrm{Mpc} < \lambda_{\mathrm{FS}} < 0.5\ \mathrm{Mpc}$ of DM would be of interest since it can be consistent with the nonvanishing matter power spectrum at large scales and avoid too many satellites of the Milky Way sized halo [14,28,40,41].

Given the problem and one of the answers to it described above, the next question naturally thrown from the particle physics side could be probably whether a well-motivated extension of the SM can accommodate such a sub-keV degenerate fermion WDM. In this work, we give our special attention to an extension of the SM with a gauged $U(1)_{\mathrm{B\text{-}L}}$ symmetry. On top of SM particle contents, in its minimal form, the model contains two heavy right-handed neutrinos ($\bar{N}_{i=1,2}$) and a complex scalar (Φ) for breaking $U(1)_{\mathrm{B\text{-}L}}$. By means of this basic setting, the model is expected to accomplish the successful explanation for the small neutrino masses via a seesaw mechanism [42–44] and the baryon asymmetry via the thermal leptogenesis [45]. Now, for the purpose of making the theory anomaly free and accommodating a nonthermal sub-keV fermion DM candidate, more chiral fermions are added to the model. The similar framework was studied in Refs. [46–48] under the name "Number Theory Dark Matter".

Beginning with the minimal set of new $U(1)_{\mathrm{B\text{-}L}}$ charged particle contents relative to the SM, we shall search for all the possible sub-keV fermion DM production mechanisms and check consistency with the Lyman-α forest observation. We gradually move to the next minimal scenario whenever an inconsistency is detected. Finally, we arrive at scenarios where multiple fundamental questions of small neutrino masses, baryon asymmetry, and DM resolving a small scale could be dealt with at once. We shall test consistency with Lyman-α forest data by computing the free-streaming length of DM and constructing a map between the thermal WDM mass and our sub-keV fermion DM mass. As an additional consistency check, we compute $\Delta N_{\mathrm{eff}}^{\mathrm{BBN}}$ contributed by the sub-keV fermion DM and "would-be" temperature today of the DM candidate.

II. MODEL

As the starting point of the task to extend the SM in a minimal way, we introduce a gauged $U(1)_{\mathrm{B\text{-}L}}$ symmetry. As the most elegant way of explaining the small neutrino masses, the seesaw mechanism predicts the presence of heavy right-handed neutrinos [42–44]. The advantage of extending the gauge symmetry group of the SM by including the gauged $U(1)_{\mathrm{B\text{-}L}}$ lies in precisely this point. The theory can be naturally rendered gauge anomaly free when there exist three right-handed neutrinos with the opposite lepton number to that of active neutrinos. The other remarkable consequence that immediately follows here is that the presence of the heavy right-handed neutrinos can help us understand the imbalance between baryon and antibaryon abundance. Induced by the out-of-equilibrium decay of the right-handed neutrino, the primordial lepton asymmetry can be converted into baryon asymmetry by sphaleron transition [45].

Motivated by these attractive aspects, we consider a variant of the SM with the gauge symmetry group $\mathrm{G_{gauge}} = \mathrm{SU(3)}_c \times \mathrm{SU(2)}_L \times \mathrm{U(1)}_Y \times \mathrm{U(1)}_{\mathrm{B\text{-}L}}$. Concerning the particle contents of the model, we begin with SM particle contents plus only two right-handed neutrinos, which is the most economical addition for the seesaw mechanism and the successful thermal leptogenesis [49]. In addition, we introduce one complex scalar to the model of which the vacuum expectation value (VEV) causes the spontaneous breaking of $U(1)_{\mathrm{B\text{-}L}}$. Via the Majorana Yukawa coupling, the complex scalar imposes masses to the two right-handed neutrinos on $U(1)_{\mathrm{B\text{-}L}}$ breaking. Of course, one is naturally tempted to make an introduction of three right-handed neutrinos at the moment since it can satisfy the anomaly-free condition of $U(1)_{\mathrm{B\text{-}L}}$ and simultaneously may be able to explain DM by taking the lightest right-handed neutrino (sterile neutrino) as a candidate of the dark matter.[4] However, there is no natural and convincing reason for such a large mass disparity between the first two and the

[2]The quantum pressure of the ultralight bosonic dark matter supported by Heisenberg's uncertainty principle can help the self-gravitating system achieve stability against gravitational collapse.

[3]The self-interaction helps efficient heat conduction from the outer more energetic DM particles to the inner colder ones, which leads to the redistribution of energy and angular momentum of DM particles. Consequently, as was shown in relevant simulations [25,26], the central halo becomes less dense compared to the CDM case and a cored halo profile forms accordingly.

[4]Indeed, this scheme has been discussed in many literatures (see, e.g., [50–52])

TABLE I. $U(1)_{\text{B-L}}$ charge assignment to the SM lepton $SU(2)_L$ doublets and singlets, two right-handed neutrino Weyl fields ($\bar{N}^{(i=1,2)}$), and the new complex scalar (Φ_{-2}). The superscript and subscript are denoting the generation and $U(1)_{\text{B-L}}$ charge, respectively.

	$L^{(1)}$	$L^{(2)}$	$L^{(3)}$	$\bar{e}_R$	$\bar{\mu}_R$	$\bar{\tau}_R$	$\bar{N}^{(1)}$	$\bar{N}^{(2)}$	Φ_{-2}
$Q_{\text{B-L}}$	-1	-1	-1	$+1$	$+1$	$+1$	$+1$	$+1$	-2

last right-handed neutrinos. Therefore, assuming only two right-handed neutrinos for the seesaw mechanism and the thermal leptogenesis, we need to find another way to accommodate the DM candidate in the model. For this purpose, recalling the necessity for making the model $U(1)_{\text{B-L}}$ anomaly free is of a great help. What could help to render $U(1)_{\text{B-L}}$ anomaly free on behalf of the third right-handed neutrino? Looking at the anomaly-free condition for $U(1)_{\text{B-L}}$ given in Eq. (1) below,[5]

$$\sum_i (Q_{\text{B-L},i})^3 = 0, \sum_i Q_{\text{B-L},i} = 0, \tag{1}$$

where the sum is over fermions charged under $U(1)_{\text{B-L}}$, and referring to Table I, one comes to realize that a new set of fermions to be added to the model should satisfy

$$\sum_i (Q_{\text{B-L},j})^3 = +1, \qquad \sum_i Q_{\text{B-L},j} = +1, \tag{2}$$

where the sum is over a new set of fermions. Here, the solutions including vectorlike fermions are out of our interest. Probing the cases to meet the two conditions in Eq. (2) simultaneously leads us to the conclusion that minimum number of the new chiral fermions to be added is four.[6] In effect, the similar logic was studied in [46,47] and diverse combinations of possible $Q_{\text{B-L}}$ values were found there. Given many options, for our work, we choose $Q_{\text{B-L}}$ assignments shown in Table II for the new chiral fermions.

Now the $U(1)_{\text{B-L}}$ charge assignment given in Tables I and II leads to the following renormalizable Yukawa couplings between Φ_{-2} and the fermions in the model charged under $U(1)_{\text{B-L}}$:

$$\mathcal{L}_{\text{Yuk}} = \sum_{i=2}^{3} \frac{1}{2} y_{N,ij} \Phi_{-2} \bar{N}^{(i)} \bar{N}^{(i)} + y_1 \Phi_{-2}^* \psi_{-9} \psi_7 + y_2 \Phi_{-2} \psi_{-5} \psi_7 + \text{H.c.} \tag{3}$$

[5]The first one is for the cancellation of the $U(1)^3_{\text{B-L}}$ anomaly and the second one is for the cancellation of the gravitational $U(1)_{\text{B-L}} \times [\text{gravity}]^2$ anomaly. The anomalies of $U(1)_{\text{B-L}} \times [\text{SM gauge interactions}]^2$ are canceled by the quark-sector contributions.

[6]Because of the Fermat's theorem, solutions with two additional Weyl fields do not exist. Solutions with three extra Weyl fields always contain two vectorlike fermions.

TABLE II. $U(1)_{\text{B-L}}$ charge assignment to the new chiral fermions to be added to the model. The subscript is denoting the $U(1)_{\text{B-L}}$ charge assigned to each.

	ψ_{-9}	ψ_{-5}	ψ_7	ψ_8
$Q_{\text{B-L}}$	-9	-5	$+7$	$+8$

Once $U(1)_{\text{B-L}}$ is spontaneously broken by the acquisition of the VEV ($\langle \Phi_{-2} \rangle \equiv V_{\text{B-L}}$) of Φ_{-2}, there arise mass eigenstates ψ_7, χ and ξ with

$$\chi \equiv \frac{y_1}{\sqrt{y_1^2 + y_2^2}} \psi_{-9} + \frac{y_2}{\sqrt{y_1^2 + y_2^2}} \psi_{-5},$$
$$\xi \equiv \frac{-y_2}{\sqrt{y_1^2 + y_2^2}} \psi_{-9} + \frac{y_1}{\sqrt{y_1^2 + y_2^2}} \psi_{-5}. \tag{4}$$

Here χ and ψ_7 form a Dirac fermion $\Psi_{\text{H}} \equiv (\chi, \psi_7^*)^{\text{T}}$ with a mass $m_{\Psi_{\text{H}}} \simeq \sqrt{y_1^2 + y_2^2} V_{\text{B-L}}$. χ and ξ are assigned *effective* $U(1)_{\text{B-L}}$ charges

$$Q_\chi = \frac{-5y_2^2 - 9y_1^2}{y_1^2 + y_2^2}, \qquad Q_\xi = \frac{-5y_1^2 - 9y_2^2}{y_1^2 + y_2^2}. \tag{5}$$

Interestingly, ψ_8 is never mixed with other fermions in the model because the $Q_{\text{B-L}}$'s of both ψ_8 and Φ_{-2} are even while those of other fermions are odd. This makes $U(1)_{\text{B-L}}$ broken down to the residual $Z_2^{\text{B-L}}$ under which all fermions except for ψ_8 are odd. Thus, ψ_8 is perfectly stable. In accordance with this observation, we take ψ_8 as the DM candidate in our model. We attribute the stability of DM to even $Q_{\text{B-L}}$ of ψ_8 from now on. ψ_8 obtains its mass via a higher dimensional operator

$$\frac{\kappa}{2} M_P \left(\frac{\Phi_{-2}}{M_P}\right)^8 \psi_8 \psi_8 \Rightarrow m_{\text{DM}} = \kappa \times \left(\frac{V_{\text{B-L}}}{10^{15}\ \text{GeV}}\right)^8 \text{eV}, \tag{6}$$

where κ is a dimensionless coefficient. Here we see that the $U(1)_{\text{B-L}}$ breaking scale directly determines the DM mass.[7]

To estimate the mass of ξ, we can try to figure out the smallest mass eigenvalue in terms of $V_{\text{B-L}}/M_P$ by writing down the 4×4 mass matrix for the fermion field vector $\vec{F} \equiv (\psi_{-9}, \psi_{-5}, \psi_7, \bar{N}^{(i)})$ formed by not only renormalizable, but also higher dimensional operators consistent with assumed symmetries. Particularly, owing to the terms[8]

[7]In this work, we assume a sufficient suppression of another higher dimensional operator of the form $\sim \Phi_{-2}^8 \Phi_{16}/M_P^5$ so that $V_{16} = 0$ can be realized when $m_{16}^2 > 0$ is chosen. This assumption makes m_{DM} totally determined by $V_{\text{B-L}}$.

[8]We omit the dimensionless coefficients for the notational simplicity.

$$\mathcal{L} = \Phi_{-2}\bar{N}^{(i)}\bar{N}^{(i)} + \frac{\Phi^{*\,2}_{-2}}{M_P}\psi_{-5}\bar{N}^{(i)}, \tag{7}$$

the mass of ξ is given by

$$m_\xi \simeq 8.7 \times 10^7 \times \left(\frac{V_{\text{B-L}}}{10^{15}}\right)^3 \text{ GeV}. \tag{8}$$

Interestingly, we obtained the small mass of the dark matter in the sub-keV regime,

$$m_{\text{DM}} \simeq 0.3 \text{ keV}, \tag{9}$$

for $V_{\text{B-L}} \simeq 2 \times 10^{15}$ GeV owing to its $B - L$ charge. Then, m_ξ becomes as large as $\sim\mathcal{O}(10^9)$ GeV.

III. SUB-keV FERMION DARK MATTER PRODUCTION FROM SCATTERING OF SM PARTICLES?: MAYBE NOT

In the previous section, we discussed a well-motivated minimal extension of the SM in which sub-keV fermion DM may arise. As was pointed out in the Introduction, we go through the procedure to check cosmological history and the free-streaming length of the DM candidate in the model in order to see whether the minimal model is good enough to be consistent with cosmological constraints including Lyman-α forest data. If not, we would gradually move to a next-to-minimal model by enlarging particle contents. From this place, since we are interested in the sub-keV DM mass regime, we assume $V_{\text{B-L}} \simeq (2-3) \times 10^{15}$ GeV based on Eq. (6), which is also consistent with the observed neutrino masses.

In the minimal model, the only particle that is communicating with ψ_8 at the renormalizable level is the $U(1)_{\text{B-L}}$ gauge boson (A'_μ). Thus, the only way for ψ_8 to be produced is pair production resulting from scattering among the SM particles via the virtual $U(1)_{\text{B-L}}$ gauge boson exchange.[9] The corresponding Feynman diagram is shown in Fig. 1. This production, however, should proceed with $\Gamma(\text{SM} + \text{SM} \to \psi_8 + \psi_8) < H$ at the reheating era. Otherwise, ψ_8 is thermalized by the SM thermal bath to become the thermal WDM which cannot have a sub-keV mass regime. Thus, we require

$$\Gamma \simeq \frac{T^5_{\text{RH}}}{V^4_{\text{B-L}}} \lesssim \frac{T^2_{\text{RH}}}{M_P} \simeq H \Rightarrow T_{\text{RH}} \lesssim \left(\frac{V^4_{\text{B-L}}}{M_P}\right)^{1/3} \simeq 10^{14} \text{ GeV}. \tag{10}$$

[9]This way of nonthermal production of the DM pair is similar to the production mechanism of DM discussed in Refs. [46,52,53]. Particularly for the relevant Boltzmann equation solution, we refer the readers to [53].

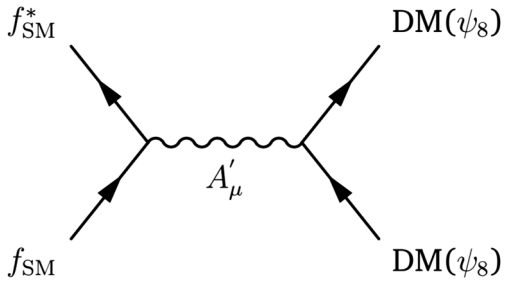

FIG. 1. DM (ψ_8) production from s-channel SM fermion scattering via the $U(1)_{\text{B-L}}$ gauge boson A'_μ exchange.

For this production route, which is most efficient at the reheating era, with the assumption that ψ_8 is identified as the sole DM component today, the DM number density to entropy density ratio reads [52]

$$Y_{\text{DM}} \equiv \frac{n_{\text{DM}}}{s_{\text{SM}}} \sim \left.\frac{n_{f_{\text{SM}}}\Gamma/H}{s_{\text{SM}}}\right|_{T=T_{\text{RH}}} \sim 6.3 \times 10^{-7}\left(\frac{g_*}{100}\right)^{-3/2} \times \left(\frac{V_{\text{B-L}}}{3 \times 10^{15} \text{ GeV}}\right)^{-4}\left(\frac{T_{\text{RH}}}{10^{13} \text{ GeV}}\right)^3, \tag{11}$$

where $n_{f_{\text{SM}}} \sim T^3$ is the SM fermion number density, $\Gamma \equiv n_{f_{\text{SM}}}\langle\sigma v\rangle$ is the interaction rate for scattering among SM fermions, g_* is the effective number of relativistic degrees of freedom, and $s_{\text{SM}} = 2\pi^2 g_* T^3/45$ is the entropy density. We assume the mass of A'_μ is greater than a reheating temperature so that A'_μ is never present in the SM thermal bath. Now the use of Eq. (11) and $Y_{\text{DM}} \equiv n_{\text{DM}}/s_{\text{SM}} \simeq 4.07 \times 10^{-4} \times (m_{\text{DM}}/1 \text{ keV})^{-1}$ along with Eq. (6) above yields[10]

$$3.9 \times 10^{-3} \simeq \left(\frac{g_*}{100}\right)^{3/2}\left(\frac{T_{\text{RH}}}{10^{13} \text{ GeV}}\right)^{-3}\left(\frac{m_{\text{DM}}}{1 \text{ keV}}\right)^{-1/2}\frac{1}{\sqrt{\kappa}}. \tag{13}$$

In other words, for a given m_{DM}, the T_{RH} required for the production of the correct amount of DM abundance today via scattering among SM fermions must be

$$T_{\text{RH}} \simeq 6.4 \times 10^{13} \times \left(\frac{g_*}{100}\right)^{1/2}\left(\frac{m_{\text{DM}}}{1 \text{ keV}}\right)^{-1/6}\left(\frac{1}{\kappa}\right)^{1/6} \text{ GeV}. \tag{14}$$

[10]From $\Omega_{\text{DM},0} = 0.24$, $H_0 = 70$ km/ sec /Mpc and $s_{\text{SM},0} \simeq 2.945 \times 10^{-11}$ eV^3 (entropy density today), DM abundance $Y_{\text{DM}} \equiv n_{\text{DM}}/s_{\text{SM}}$ is expressed in terms of DM mass as

$$Y_{\text{DM}} \equiv \frac{n_{\text{DM}}}{s_{\text{SM}}} \simeq 4.07 \times 10^{-4} \times \left(\frac{m_{\text{DM}}}{1 \text{ keV}}\right)^{-1}, \tag{12}$$

at DM production time.

For $g_* \simeq 100$, $m_{\rm DM} \simeq \mathcal{O}(100)$ eV and $\kappa \simeq \mathcal{O}(1)$, $T_{\rm RH}$ in Eq. (14) reads $\sim\mathcal{O}(10^{13})$ GeV. Provided that the right amount of DM is produced at the reheating era with this reheating temperature, we also expect the production of ξ via the similar SM scattering with the production ratio

$$\frac{\Gamma(\mathrm{SM}+\mathrm{SM}\to\xi+\xi)}{\Gamma(\mathrm{SM}+\mathrm{SM}\to\psi_8+\psi_8)} \simeq \frac{Q_\xi^2}{Q_{\psi_8}^2} = \left(\frac{-5y_1^2-9y_2^2}{8y_1^2+8y_2^2}\right)^2. \tag{15}$$

On production, we anticipate that ξ completes decaying to the SM Higgs and lepton before the electroweak (EW) symmetry breaking time is reached and so it is cosmologically harmless (for details, see Appendix A). Because of the small interaction rate, ψ_8 starts free-streaming since production near the reheating era. The free-streaming length must be checked to be at least smaller than 0.5 Mpc. This is for avoiding too much suppression of the matter power spectrum on small scales inconsistent with observation.

The free-streaming length of DM is computed by

$$\begin{aligned}\lambda_{\rm FS} &= \int_{t_p}^{t_0} \frac{\langle v_{\rm DM}(t)\rangle}{a}\mathrm{d}t \\ &\simeq \int_{a_p}^{1} \frac{1}{H_0\sqrt{\Omega_{\rm rad,0}+a\Omega_{\rm m,0}}} \\ &\quad\times \frac{\langle p_{\rm DM}(a_p)\rangle a_p}{\sqrt{(\langle p_{\rm DM}(a_p)\rangle a_p)^2+m_{\rm DM}^2 a^2}}\mathrm{d}a\end{aligned} \tag{16}$$

where t_p and a_p are the time and the scale factor at which DM starts free streaming, $\langle v_{\rm DM}(t)\rangle$ is the average velocity of the dark matter at the time t, and $\langle p_{\rm DM}(a_p)\rangle$ is the DM momentum at t_p. $\Omega_{\rm rad,0}$ and $\Omega_{\rm m,0}$ denote the radiation and matter density parameters, respectively. Even if ψ_8 does not form a dark thermal bath, its momentum distribution is expected to be similar to the thermal distribution since it is produced from the scattering of SM fermions which are in the thermal bath. The average momentum of the DM is estimated as

$$\langle p_{\rm DM}(a_p)\rangle \gtrsim 3.15\times T_{\rm RH}, \tag{17}$$

where $a_p = a_{\rm RH} \simeq (10^{-13}\ \mathrm{GeV})/T_{\rm RH}$ is the time of the onset of the DM free streaming.[11] The factor 3.15 applies for the typical thermal distribution of fermions. Using Eq. (17), the estimation of $\lambda_{\rm FS}$ for even $m_{\rm DM} = 1$ keV yields 1.25 Mpc. The smaller DM mass corresponds to the longer $\lambda_{\rm FS}$ than this. This estimation concludes that the minimal scenario cannot produce a degenerate sub-keV fermion DM candidate for explaining the cored DM profiles for dSphs.

Then, what is another way that could be considered to produce sub-keV fermion DM with a shorter free-streaming length? We notice that decreasing $T_{\rm RH}$ cannot shorten $\lambda_{\rm FS}$ in Eq. (16) as long as $T_{\rm RH} \gtrsim 10$ MeV where 10 MeV is the lower bound of $T_{\rm RH}$ from the big bang nucleosynthesis (BBN). On the other hand, because ψ_8 cannot be coupled to any particle in the model other than the $U(1)_{\rm B\text{-}L}$ gauge boson at the renormalizable level,[12] no other DM production mechanism can be envisioned in the minimal model. Hence, we cannot help but conclude that $\lambda_{\rm FS}$ cannot be shortened unless another DM production mechanism is considered by modifying the minimal model.

Therefore, we conclude that ψ_8 produced from the SM particle scattering cannot be a candidate for the degenerate sub-keV DM to resolve the core-cusp problem. Now the whole of reasoning we followed in Sec. III necessitates searching for a new way of producing DM which we discuss in the next section.

IV. SUB-keV FERMION DM FROM INFLATON DECAY

As a next step, let us consider the DM production from the inflaton decay. ψ_8 can be coupled to the inflaton via

$$\mathcal{L} \sim \frac{\Phi_I}{M_P}\psi_8^\dagger \bar{\sigma}^\mu D_\mu \psi_8, \tag{18}$$

where Φ_I is the inflaton field and is assumed to be a gauge singlet and Lorentz scalar from here on. If the mass of the B-L gauge boson, $m_{\rm B\text{-}L}$, is larger than the inflaton mass, i.e., $m_{\rm B\text{-}L} > m_I$, the decay rate of the process $\Phi_I \to \psi_8 + \psi_8^\dagger +$ B-L charged particles (X) is

$$\Gamma(\Phi_I \to \psi_8 + \psi_8^\dagger + X) \sim \frac{m_I^7}{M_P^2 V_{\rm B\text{-}L}^4}. \tag{19}$$

To explain the current abundance of the dark matter, one requires

$$\frac{m_I^7}{M_P^2 V_{\rm B\text{-}L}^4} \sim \frac{T_{\rm RH}^2}{M_P}\mathrm{Br} \sim \frac{T_{\rm RH} m_I}{M_P}10^{-4}\left(\frac{m_{\rm DM}}{1\ \mathrm{keV}}\right)^{-1}, \tag{20}$$

where Br is the branching ratio of $\Phi_I \to \psi_8 + \psi_8^\dagger + X$ to the inflaton decay rate.[13] The reheating temperature is

[11] Here we use $a_{\rm EW}(a_{\rm EW}) = a_{\rm RH}T_{\rm RH}$ with $a_{\rm EW} \simeq 10^{-15}$ and $T(a_{\rm EW}) \simeq 100$ GeV.

[12] Note that ψ_8 cannot have a renormalizable coupling to a gauge singlet inflaton that satisfies gauge and Lorentz invariance all together.

[13] For the third relation, the branching ratio is determined to provide the current dark matter density [refer to the discussion around Eq. (31)].

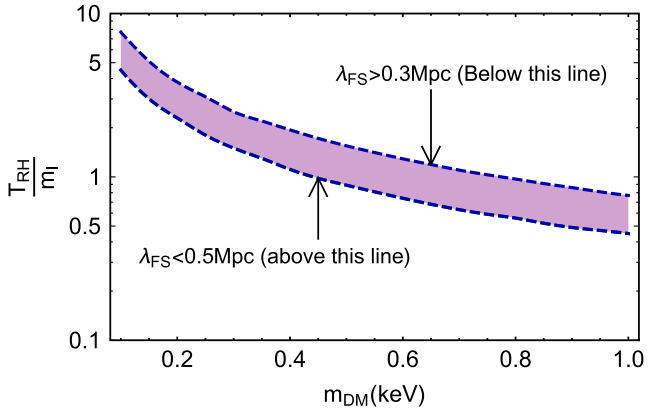

FIG. 2. The ratio of a reheating temperature ($T_{\rm RH}$) to an inflaton mass (m_I) that results in DM's free-streaming length 0.3 Mpc $<\lambda_{\rm FS}<$ 0.5 Mpc when DM is directly produced from the inflaton decay.

$$T_{\rm RH}\sim 10^4 m_I\frac{m_I^5}{M_P V_{\rm B\text{-}L}^4}\left(\frac{m_{\rm DM}}{1\ {\rm keV}}\right). \tag{21}$$

To avoid the dominant production from the SM thermal bath (the case discussed in Sec. III), $T_{\rm RH}\lesssim 10^{13}$ GeV is required. In addition, the ratio of a reheating temperature ($T_{\rm RH}$) to an inflaton mass (m_I) that results in DM's free-streaming length 0.3 Mpc $<\lambda_{\rm FS}<$ 0.5 Mpc is $\mathcal{O}(0.1)$–$\mathcal{O}(1)$ as can be seen in Fig. 2 when DM is directly produced from the inflaton decay with $\langle p_{\rm DM}(a_p)\rangle = m_I/2$ and $a_p = a_{\rm RH}$. However, this ratio from Eq. (21) for $T_{\rm RH}\lesssim 10^{13}$ GeV leads to

$$T_{\rm RH}\ll m_I, \tag{22}$$

which is inconsistent with Fig. 2. Thus, this possibility is out of our interest.

On the other hand, for $m_{\rm B\text{-}L}<m_I$, the decay rate is

$$\Gamma(\Phi_I\to\psi_8+\psi_8^\dagger+A'_\mu)\sim g_{\rm B\text{-}L}^2 m_I\left(\frac{m_I}{M_P}\right)^2, \tag{23}$$

where $g_{\rm B\text{-}L}$ denotes the B-L gauge coupling. To explain the dark matter density, we require

$$g_{\rm B\text{-}L}^2 m_I\left(\frac{m_I}{M_P}\right)^2\sim 10^{-4}\frac{T_{\rm RH}m_I}{M_P}\left(\frac{m_{\rm DM}}{1\ {\rm keV}}\right)^{-1}. \tag{24}$$

This leads to

$$T_{\rm RH}\sim 10^4 g_{\rm B\text{-}L}^2 m_I\left(\frac{m_I}{M_P}\right)\left(\frac{m_{\rm DM}}{1\ {\rm keV}}\right). \tag{25}$$

Similar to Eq. (21), Eq. (25) gives rise to

$$T_{\rm RH}\ll m_I, \tag{26}$$

which is inconsistent with Fig. 2. Thus, this possibility is also out of our interest.[14]

Therefore, we need to extend the minimal model to have the degenerate fermion DM. As we will explain in detail, one simple possibility is to introduce a complex scalar field Φ_{16} with $Q_{\rm B\text{-}L}=16$. This scalar field couples to DM through

$$\mathcal{L}=y_*\Phi_{16}^*\psi_8\psi_8, \tag{27}$$

where y_* is a dimensionless coupling.[15]

The renormalizable scalar sector potential we consider in the following reads[16]

$$V_{\rm scalar}=+m_{16}^2|\Phi_{16}|^2+\frac{\lambda_{16}}{4}|\Phi_{16}|^4+g\Phi_I|\Phi_{16}|^2 + V(\Phi_I)+V(H), \tag{28}$$

where m_{16} is a parameter with a mass dimension, λ_{16} is a dimensionless coupling, g is a parameter with a mass dimension, and $V(\Phi_I)$ and $V(H)$ are the potentials for inflaton and the SM Higgs doublet. We take $\langle\Phi_{16}\rangle=0$ in the vacuum, assuming the Φ_{16} has a positive mass squared, $m_{16}^2>0$. This makes Eq. (6) intact.[17] In Sec. IV, we assume that the Hubble induced mass squared for the Φ_{16} is positive so that Φ_{16} sits near the origin of the field space during and in the end of inflation.

[14]Along with Eq. (26), a too large a mass value itself for the inflaton also makes ψ_8 production from the inflaton decay with $m_{\rm B\text{-}L}<m_I$ not viable. From Fig. 2 and $m_{\rm B\text{-}L}<m_I$, we obtain $m_{\rm B\text{-}L}<m_I\sim(\mathcal{O}(0.1)-\mathcal{O}(1))T_{\rm RH}$ to have a degenerate fermion DM. If A'_μ produced from the process $\Phi_I\to\psi_8+\psi_8^\dagger+A'_\mu$ joins the SM thermal bath, ψ_8 would do so as well via the inverse decay process of A'_μ and becomes the thermal WDM. Thus, we demand $\Gamma(A'_\mu\to\psi_8+\psi_8^\dagger)<H$ for $T_{\rm SM}\simeq m_{\rm B\text{-}L}$. In conjunction with Eq. (25) and the condition $m_I\sim(\mathcal{O}(0.1)$–$\mathcal{O}(1))T_{\rm RH}$, this requirement gives $m_I\sim\mathcal{O}(10^{15})$–$\mathcal{O}(10^{16})$ GeV of which a corresponding inflation model is difficult to find.

[15]Similar to ψ_8, Φ_{16} could be produced from SM particle scattering as long as $T_{\rm RH}$ is large enough. The relevant diagram would be the one in Fig. 1 with ψ_8 replaced by Φ_{16}. For this route, due to $Q_{\rm B\text{-}L}$ ratio, we expect four times more production of Φ_{16} than that of ψ_8. This case is also out of our interest because a significant amount of DM (∼25%) would travel too large a free-streaming length as shown above using Eqs. (16) and (17).

[16]For the purpose of preventing Φ_{16} from being thermalized by any particle, we assume sufficiently suppressed renormalizable mixing of Φ_{16} with other scalars like $\sim(H^\dagger H)|\Phi_{16}|^2$, $\sim|\Phi_{-2}|^2|\Phi_{16}|^2$ and $\sim|\Phi_I|^2|\Phi_{16}|^2$ which are allowed by symmetries in the model. See Appendix. B for more discussion about the Higgs portal couplings.

[17]For the case where $m_{16}^2<0$ to induce a nonzero VEV of Φ_{16}, we find that one needs to focus on a large enough value of V_{16}, otherwise the phase component of Φ_{16} and ψ_8 can easily join the dark thermal bath at the reheating era. This precludes our goal of producing the nonthermally originated ψ_8 as the WDM candidate. Thus, we restrict ourselves to the case with $V_{16}=0$ by choosing $m_{16}^2>0$.

Now Φ_{16} may be produced from the inflaton decay at the reheating era via the decay operator $\sim g\Phi_I|\Phi_{16}|^2$ if $m_I \gtrsim 2m_{16}$ holds. In this section, we attend to the Φ_{16} particle produced in this manner. We are aiming to show that such a Φ_{16} could be a mother particle producing sub-keV fermion DM (ψ_8) consistent with the Lyman-α forest observation. Depending on a value of λ_{16}, we have two different scenarios. We explore a case where a dark sector thermal bath forms in Sec. IV A and the other case where a dark sector thermal bath *never* forms in Sec. IV B.

A. The case with formation of dark sector thermal bath

In this section, we consider the case in which a dark thermal bath purely made up of Φ_{16} forms when Φ_{16} is produced from the inflaton decay. When $\lambda_{16} \neq 0$ holds, from the comparison

$$\Gamma \simeq \lambda_{16}^2 T_D \gtrsim \frac{T_{\rm SM}^2}{M_P} \simeq H \Rightarrow x\lambda_{16}^2 M_P \gtrsim T_{\rm SM}, \quad (29)$$

where T_D is the temperature in the dark sector, we realize that it is easy for a dark thermal bath made up of Φ_{16} to form as long as the quartic interaction (λ_{16}) of Φ_{16} is not too small. Here $x = T_D/T_{\rm SM}$ is a fraction of order $\mathcal{O}(0.1)$ to be determined by DM relic density matching. We define the branching ratio Br to satisfy $n_{16} = {\rm Br} \times n_I \simeq {\rm Br} \times (\rho_{\rm SM}/m_I)$[18] where n_{16} and n_I are the number density of Φ_{16} and inflaton (Φ_I), respectively. We assume $\rho_{\rm I} \simeq \rho_{\rm SM}$ at the reheating era. From the number density comparison, we obtain the relation between dark sector temperature and SM sector temperature

$$T_{\rm D}(a_{\rm RH}) \simeq 5.2 \times {\rm Br}^{1/3} \times \frac{T_{\rm RH}^{4/3}}{m_I^{1/3}} \simeq 0.34 \times \left(\frac{m_{\rm DM}}{1\ {\rm keV}}\right)^{-1/3} \times T_{\rm RH}, \quad (32)$$

where we used $g_{\rm D}(a_{\rm RH}) = 2$ and $g_{\rm SM}(a_{\rm RH}) = 106.75$. The second equality is coming from Eq. (31). The ratio of $T_{\rm D}/T_{\rm SM}$ remains the same until Φ_{16} decays to a DM pair. We note that Br is lower bounded as ${\rm Br} \gtrsim (2.7 \times 10^{-4}(m_{\rm DM}/1\ {\rm keV})^{-1})^2$. This constraint is derived from the condition that Φ_{16} never gets into the SM thermal bath by the decay and the inverse decay process of $\Phi_I \leftrightarrow \Phi_{16} + \Phi_{16}^*$, and the requirement of obtaining the correct DM density [see Eq. (31)].[19]

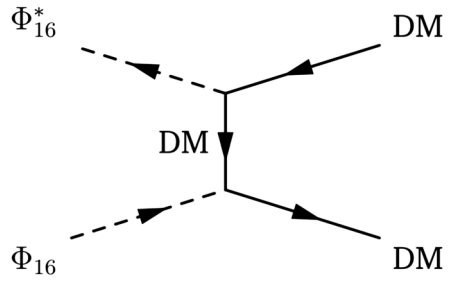

FIG. 3. The scattering among two Φ_{16}'s to produce a pair of DM via the t-channel DM exchange.

Concretely, we consider a scenario in which Φ_{16} becomes nonrelativistic in the dark thermal bath before the time of $\Gamma(\Phi_{16} \to \psi_8 + \psi_8) \simeq H$ is reached. Afterwards, nonrelativistic Φ_{16} decays to the DM pair when the time of $\Gamma(\Phi_{16} \to \psi_8 + \psi_8) \simeq H$ is reached. The similar scenario was considered in [48,54]. We argue that DM does not exist at the reheating era and is produced only from the decay of Φ_{16}. To this end, we define $T_{{\rm SM},i}$ ($T_{{\rm D},i}$) to be the SM (dark) thermal bath temperature at which $\Gamma_i \simeq H$ holds. For $\Phi_{16} + \Phi_{16}$ scattering to produce DM + DM and vice versa via the t-channel DM exchange shown in Fig. 3, the interaction rate reads

$$\Gamma_1 \simeq y_*^4 T_{\rm D,1}, \quad T_{\rm SM,1} \simeq 0.34 \times \left(\frac{m_{\rm DM}}{1\ {\rm keV}}\right)^{-1/3} \times y_*^4 M_P,$$
$$T_{\rm D,1} \simeq 0.34^2 \times \left(\frac{m_{\rm DM}}{1\ {\rm keV}}\right)^{-2/3} \times y_*^4 M_P, \quad (33)$$

where y_* is Yukawa between Φ_{16} and DM. For Φ_{16} decay to DM + DM, the decay rate (when $m_{16} > T_{\rm DS}$) is given by

$$\Gamma_2 \simeq \frac{y_*^2}{8\pi} m_{16}, \quad T_{\rm SM,2} \simeq \frac{y_*}{5}\sqrt{m_{16} M_P},$$
$$T_{\rm D,2} \simeq 0.34 \times \left(\frac{m_{\rm DM}}{1\ {\rm keV}}\right)^{-1/3} \times \frac{y_*}{5}\sqrt{m_{16} M_P}, \quad (34)$$

where m_{16} is the mass of Φ_{16}.

To realize the scenario as we wish, we need to demand

$$m_{16} > T_{\rm D,2} \quad \text{and} \quad m_{16} > T_{\rm D,1}. \quad (35)$$

From the first inequality in Eq. (35), we obtain

[18]This relation $n_{16} \simeq {\rm Br} \times (\rho_{\rm SM}/m_I)$ can be used to derive the relation between m_I, $T_{\rm RH}$ and Br. Using the approximation $2n_{\phi_{16}} = n_{\rm DM}$ at production time, one obtains

$$Y_{\rm DM} \equiv \frac{n_{\rm DM,0}}{s_{\rm SM,0}} \simeq \left.\frac{2n_{\phi_{16}}}{s_{\rm SM}}\right|_{T=T_{\rm RH}} \simeq 2{\rm Br}\left.\frac{\rho_{\rm SM}}{m_I s_{\rm SM}}\right|_{T=T_{\rm RH}}. \quad (30)$$

Using Eqs. (12) and (30), one obtains

$${\rm Br}\frac{T_{\rm RH}}{m_I} \simeq 2.7 \times 10^{-4} \times \left(\frac{m_{\rm DM}}{1\ {\rm keV}}\right)^{-1}. \quad (31)$$

[19]The condition is ${\rm Br} \times T_{\rm RH}^2/M_P \lesssim m_I^2/M_P$ where the process $\Phi_I \leftarrow \Phi_{16} + \Phi_{16}^*$ is ineffective until the inflaton becomes nonrelativistic and disappears.

$$y_* < 14.7 \times \left(\frac{m_{\rm DM}}{1\ {\rm keV}}\right)^{1/3} \sqrt{\frac{m_{16}}{M_P}} \equiv y_{*,\rm max}. \quad (36)$$

From the second inequality in Eq. (35), we obtain

$$y_* < 1.7 \times \left(\frac{m_{\rm DM}}{1\ {\rm keV}}\right)^{1/6} \left(\frac{m_{16}}{M_P}\right)^{1/4}. \quad (37)$$

In addition, requiring that DMs do not form a thermal bath via their self-interaction through Φ_{16} exchanges after its production

$$\Gamma \simeq n_{\rm DM} \frac{y_*^4}{m_{16}^2} \lesssim H \quad \text{at } a = a_p \quad (38)$$

leads to the condition

$$y_* \lesssim \left(\frac{m_{16}}{M_P}\right)^{3/10} \left(\frac{m_{\rm DM}}{1\ {\rm keV}}\right)^{1/5}. \quad (39)$$

Thus, we can see that for $m_{16} \lesssim 10^{13}$ GeV, Eqs. (37) and (39) are satisfied as long as Eq. (36) is so. Together with m_{16}, y_* is treated as a free parameter as far as $y_* \lesssim y_{*,\rm max}$ is satisfied. The smaller y_* becomes, the later the time of the onset of the free streaming of DM. Given a fixed initial momentum $\langle p_{\rm DM}(a_{\rm FS})\rangle \simeq m_{16}/2$, the larger $a_{\rm FS}$ implies a larger $\langle p_{\rm DM}(a > a_{\rm FS})\rangle$ for a fixed scale factor $a > a_{\rm FS}$. In light of the fact that the late universe contribution to $\lambda_{\rm FS}$ is greater than the earlier one, we are led to speculate that for the same $(m_{16}, m_{\rm DM})$, the smaller y_* would lead to the larger $\lambda_{\rm FS}$ and hence be a more stringent constraint on $m_{\rm DM}$.

To constrain the model, we consider the free-streaming length criterion $0.3\ {\rm Mpc} < \lambda_{\rm FS} < 0.5\ {\rm Mpc}$. Following Eq. (16), the free-streaming length of DM produced from a nonrelativistic Φ_{16} is

$$\begin{aligned}\lambda_{\rm FS} &\simeq \int_{t_p}^{t_0} \frac{\langle v_{\rm DM}(t)\rangle}{a} {\rm d}t \\ &\simeq \int_{a_p}^{1} \frac{1}{H_0\sqrt{\Omega_{\rm rad,0} + a\Omega_{\rm m,0}}} \\ &\quad \times \frac{\langle p_{\rm DM}(a_p)\rangle a_p}{\sqrt{(\langle p_{\rm DM}(a_p)\rangle a_p)^2 + m_{\rm DM}^2 a^2}} {\rm d}a \\ &= \int_{a_p}^{1} \frac{1}{H_0\sqrt{\Omega_{\rm rad,0} + a\Omega_{\rm m,0}}} \frac{m_{16} a_p}{\sqrt{(m_{16}a_p)^2 + 4m_{\rm DM}^2 a^2}} {\rm d}a, \end{aligned} \quad (40)$$

where $\langle p_{\rm DM}(a_{\rm FS})\rangle \simeq m_{16}/2$ was used with $a_p \simeq a_{\rm FS}$. Here, a_p and $a_{\rm FS}$ are the scale factors at which the production of DM and the free streaming of DM take place, respectively. Using Eq. (34), a_p can be computed via

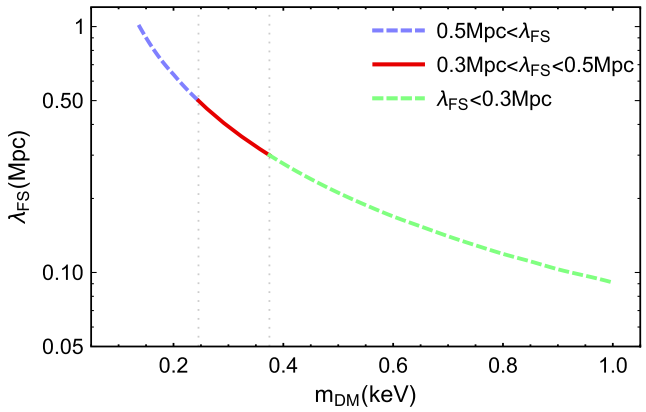

FIG. 4. Dark matter mass ($m_{\rm DM}$) vs free-streaming length ($\lambda_{\rm FS}$). For this plot, $y_* = y_{*,\rm max}$ in Eq. (36) is assumed. For each $m_{\rm DM}$, the smaller y_* yields the larger $\lambda_{\rm FS}$.

$$a_p \simeq a_{\rm FS} \simeq \frac{10^{-13}\ {\rm GeV}}{T_{\rm SM,2}} = \frac{5\times 10^{-13}\ {\rm GeV}}{y_*\sqrt{m_{16}M_P}}. \quad (41)$$

For a fixed $(m_{16}, m_{\rm DM})$, $y_{*\,\rm max}$ in Eq. (36) is determined, defining an allowed range of $y_* < y_{*,\rm max}$. Within the range, the smaller y_* results in the longer $\lambda_{\rm FS}$ since the free-streaming is delayed with the same initial momentum $\langle p_{\rm DM}(a_{\rm FS})\rangle \simeq m_{16}/2$. This means that for each set of $(m_{16}, m_{\rm DM})$, $y_* = y_{*,\rm max}$ in Eq. (41) yields the smallest $\lambda_{\rm FS}$ value. On the other hand, for $y_* = y_{*,\rm max}$, we notice that $\lambda_{\rm FS}$ in Eq. (40) becomes independent of m_{16} since $m_{16}a_p$ is so. Thus, we realize that for $y_* = y_{*,\rm max}$, $\lambda_{\rm FS}$ is minimized for each $m_{\rm DM}$ whatever m_{16} is. In Fig. 4, we show $\lambda_{\rm FS}$ computed with $y_* = y_{*,\rm max}$ for the dark matter mass range $0.1\ {\rm keV} \lesssim m_{\rm DM} \lesssim 1\ {\rm keV}$. For a smaller y_* choice, the curve in Fig. 4 would move upward. Without going through the further study with y_* smaller than $y_{*,\rm max}$, we restrict ourselves to the case with $y_* = y_{*,\rm max}$ as an example, but the logic presented below can be also applied to other values of (y_*, m_{16}) for the consistency check.

Starting with the momentum $\simeq m_{16}/2$ at $a = a_{\rm FS}$, the sub-keV DM we discuss here is still relativistic at the BBN era with the momentum $\sim\mathcal{O}(1)$ MeV. As such, the sub-keV DM serves as an extra radiation during the BBN era and therefore its contribution to $\Delta N_{\rm eff}^{\rm BBN}$ needs to be checked to be consistent with the known constraint. For each $m_{\rm DM}$, we computed $\Delta N_{\rm eff}^{\rm BBN}$ contributed by DM at the BBN era and found that the model with $y_* = y_{*,\rm max}$ is consistent with $\Delta N_{\rm eff}^{\rm BBN} \lesssim 0.114$ (95% C.L.) recently reported in [55]. For the computation of $\Delta N_{\rm eff}^{\rm BBN}$ contributed by DM, we refer the readers to Appendix C. As the final consistency check, we estimated the would-be temperature today ($\tilde{T}_{\rm DM,0}$) for ψ_8 based on Eq. (E2) which reads

$$\tilde{T}_{\rm DM,0} \simeq 3.4\times 10^{-9} \times \left(\frac{m_{\rm DM}}{1\ {\rm keV}}\right)^{-5/3} {\rm K}, \quad (42)$$

where we used $y_* = y_{*,\max}$ in Eq. (36) and $a_{\rm FS}$ in Eq. (41). We presented a brief explanation as to the necessary condition for fermion DM to be in a degenerate configuration in Appendix E. For $m_{\rm DM}$ of our interest, we see that $\tilde{T}_{\rm DM,0} < T_{\rm DEG} \simeq \mathcal{O}(10^{-4})$ K $- \mathcal{O}(10^{-3})$ K. This confirms that the current temperature of the DM becomes low enough to accomplish the degenerate configuration when the structure formation is ignored.

We notice that y_* can be constrained by $\Delta N_{\rm eff}^{\rm BBN}$, which we do not explore in detail. Intriguingly, for $y_* = y_{*,\max}$, the criterion 0.3 Mpc $\lesssim \lambda_{\rm FS} \lesssim$ 0.5 Mpc gives the mass constraint 0.25 keV $\lesssim m_{\rm DM} \lesssim$ 0.37 keV, which lies in the range of the degenerate fermion DM mass accounting for the cored DM profiles of dSphs in Refs. [28–31]. Another choice of $y_* < y_{*,\max}$ will make 0.3 Mpc $\lesssim \lambda_{\rm FS} \lesssim$ 0.5 Mpc correspond to a larger $m_{\rm DM}$ range.

Additionally, we also discuss the constraint on the mass of our DM candidate (ψ_8) mapped from a conservative lower bound for the mass of the thermal WDM, i.e., 1.9 keV (95% C.L.), recently reported in [56]. We make a detailed discussion about how the mapping can be achieved in Appendix D. Here we directly construct the map based on Eq. (D3). We begin by equating the warmness parameters for ψ_8 (σ_{ψ_8}) and the thermal WDM ($\sigma_{\rm wdm}$)

$$\sigma_{\psi_8} = \sigma_{\rm wdm} \Leftrightarrow \tilde{\sigma}_{\psi_8} \frac{T_{\psi_8}}{m_{\psi_8}} = \tilde{\sigma}_{\rm wdm} \frac{T_{\rm wdm}}{m_{\rm wdm}}, \tag{43}$$

where m and T denote a mass and temperature, and $\tilde{\sigma}$ is defined in Eq. (D2). As a particle produced from the decay of a nonrelativistic mother particle, ψ_8 is characterized by the momentum space distribution function $f(q,t) = (\beta/q)\exp(-q^2)$ where β is a normalization factor and $q \equiv p/T$ is used [57–61]. This gives us $\tilde{\sigma}_{\psi_8} \simeq 1$. On the other hand, since $m_{16} \gg m_{\rm DM}$ is assumed, DM temperature at the matter-radiation equality can be written as

$$T_{\psi_8}(a_{\rm eq}) = \frac{m_{16} a_{\rm FS}}{2 a_{\rm eq}} = 0.17 \times 10^{-7}\ \text{keV} \times \left(\frac{m_{\psi_8}}{1\ \text{keV}}\right)^{-1/3} \times (1 + z_{\rm eq}), \tag{44}$$

with $a_{\rm FS}$ defined in Eq. (41). Finally, by using $\tilde{\sigma}_{\rm wdm} = 3.6$ for the thermal WDM and $T_{\rm wdm}(a_{\rm eq}) = T_{\rm wdm,0}/a_{\rm eq}$ in Eq. (D4), we obtain the map

$$m_{\psi_8} \simeq 0.2 \times m_{\rm wdm}. \tag{45}$$

Applying the conservative constraint $m_{\rm wdm} > 1.9$ keV [56], we obtain $m_{\psi_8} \gtrsim 0.4$ keV. This result may seem a tension with $m_{\rm DM}$ required for a degenerate fermion DM in [28,29]. However, indeed there exist some uncertainties in the velocity anisotropy parameter used for the fitting of the stellar velocity dispersion, the lower bound of the Fornax dSphs halo radius, and the baryon's effect on the DM halo profile. Also, still for some dSphs other than Fornax, the best fitting for the stellar velocity dispersion is done by $m_{\rm DM}$ as large as 550–650 eV [30]. Here, without performing a detailed fitting analysis to infer the degenerate fermion DM mass, we take a conservative attitude to understand 100 eV $\lesssim m_{\rm DM} \lesssim$ 1 keV as the interesting range relating to the degenerate fermion DM solution to the core-cusp problem.

B. The case without formation of dark sector thermal bath

For the case where Φ_{16} does have a tiny or vanishing quartic interaction, Φ_{16} would not form a dark thermal bath as far as the Yukawa interaction where ψ_8 is sufficiently small. Since production from the inflaton decay, it would continue to free stream until it decays to a pair of ψ_8. Note that this early free streaming of Φ_{16} is not problematic at all for the small-scale perturbations since the early time free-streaming length is negligibly small. With this picture in mind, in this section, we study the possibility of having a degenerate fermion DM arising from the decay of a free nonrelativistic scalar Φ_{16}. We explore the parameter space of the model where the free-streaming length of ψ_8 becomes consistent with the Lyman-α forest observation.

In order to avoid having the thermal WDM, we focus on the scenario where Φ_{16} starts the free streaming once produced from the inflaton decay. After that, Φ_{16} becomes nonrelativistic first and then decays to DM pairs. Differing from the previous case with $\lambda_{16} \neq 0$, the time when Φ_{16} becomes nonrelativistic is sensitive to the inflaton mass now. Φ_{16} has momentum $p_{16}(a_{\rm RH}) \simeq m_I/2$ at the reheating era on production and then becomes nonrelativistic at

$$a = a_{\rm NR} \equiv \frac{m_I a_{\rm RH}}{2 m_{16}} \simeq \frac{m_I \times 10^{-13}\ \text{GeV}}{2 \times T_{\rm RH} \times m_{16}} \simeq \frac{\text{Br} \times \left(\frac{m_{\rm DM}}{1\ \text{keV}}\right) \times 10^{-13}\ \text{GeV}}{5.4 \times 10^{-4} \times m_{16}}, \tag{46}$$

where we used $a_{\rm RH} \simeq (10^{-13}\ \text{GeV})/T_{\rm RH}$ for the third equality and Eq. (31) for the last equality. For our purpose, we demand that

$$T_{\rm SM}(a_{\rm NR}) > T_{\rm SM,2} > T_{\rm SM,1} \tag{47}$$

where $T_{\rm SM,1}$ and $T_{\rm SM,2}$ were defined in Eq. (33) and Eq. (34). From the first inequality in Eq. (47), we obtain

$$y_* < \frac{2.7 \times 10^{-3}}{\text{Br} \times \left(\frac{m_{\rm DM}}{1\ \text{keV}}\right)} \times \sqrt{\frac{m_{16}}{M_P}} \equiv y_{*,1}. \tag{48}$$

From the second inequality in Eq. (47), we obtain

$$y_* < 0.84 \times \left(\frac{m_{\rm DM}}{1\ \text{keV}}\right)^{1/9} \left(\frac{m_{16}}{M_P}\right)^{1/6} \equiv y_{*,2}. \tag{49}$$

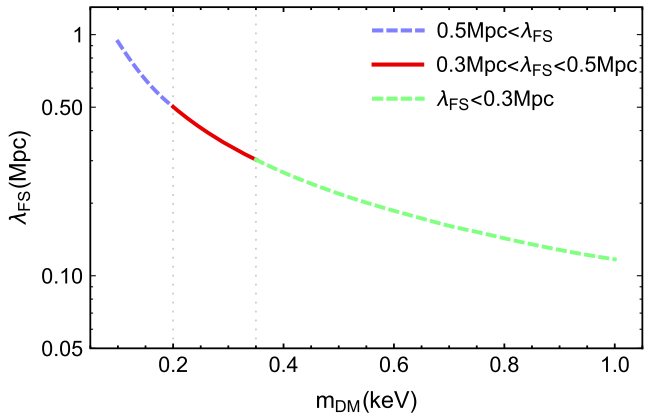

FIG. 5. Dark matter mass ($m_{\rm DM}$) vs free-streaming length ($\lambda_{\rm FS}$). For this plot, $(m_{16} = 5 \times 10^5\ {\rm GeV}, {\rm Br} = 10^{-6}, y_* = 5 \times 10^{-6})$ is assumed. For each $m_{\rm DM}$, the smaller y_* yields the larger $\lambda_{\rm FS}$.

In addition, as discussed in Sec. IV A, we require

$$y_* \lesssim \left(\frac{m_{16}}{M_P}\right)^{3/10} \left(\frac{m_{\rm DM}}{1\ {\rm keV}}\right)^{1/5} \equiv y_{*,3}, \tag{50}$$

so that the DM does not form a dark thermal bath via their self-interaction through the Φ_{16} exchange after its production.

For a given set of $(m_{16}, m_{\rm DM}, {\rm Br})$, each of $(y_{*,1}, y_{*,2}, y_{*,3})$ is to be determined. Define $y_{*,\max} \equiv \min(y_{*,1}, y_{*,2}, y_{*,3})$. Then a choice of the Yukawa coupling satisfying $y_* < y_{*,\max}$ will satisfy Eq. (47). Numerically we find that (1) for ${\rm Br} \gtrsim 10^{-3}$, $y_{*,\max} = y_{*,1}$ for any sub-keV $m_{\rm DM}$ and (2) for ${\rm Br} \lesssim 10^{-4}$, $y_{*,\max}$ is either $y_{*,1}$ or $y_{*,3}$. For a fixed $m_{\rm DM}$, $\lambda_{\rm FS}$ depends on m_{16} and y_*, and these two are inversely correlated. Thus, in principle, for a fixed $m_{\rm DM}$, a set of (m_{16}, y_*) satisfying $\lambda_{\rm FS} \in (0.3, 0.5)$ Mpc can be readily found and is consistent insofar as $y_* < y_{*,\max}$.[20] In this section, instead of probing all the allowed parameter space for $(m_{16}, {\rm Br}, y_*, m_{\rm DM})$, for our purpose it suffices to choose a specific benchmark set of parameters $(m_{16} = 5 \times 10^5\ {\rm GeV}, {\rm Br} = 10^{-6}, y_* = 5 \times 10^{-6})$ to show that a degenerate sub-keV fermion DM can be produced in the model. Then we see that $y_* < y_{*,\max}$ is satisfied. We emphasize that this example is not atypical and the following logic and consistency check can also apply for other values of parameters. The result of the computation for $\lambda_{\rm FS}(m_{\rm DM})$ is shown in Fig. 5. Interestingly, the range $0.2\ {\rm keV} \lesssim m_{\rm DM} \lesssim 0.35\ {\rm keV}$ corresponds to the criterion $0.3\ {\rm Mpc} \lesssim \lambda_{\rm FS} \lesssim 0.5\ {\rm Mpc}$ and gives the mass constraint, which lies in the range of degenerate fermion DM mass accounting for the cored DM profiles of dSphs in Refs. [28–31]. The smaller y_* and the larger m_{16} would make the curve in Fig. 5 move upward.

As the final consistency check, we compute $\Delta N_{\rm eff}^{\rm BBN}$ and the would-be temperature today for ψ_8. First, from Eqs. (41), (C2), and $y_* = 5 \times 10^{-6}$, $\Delta N_{\rm eff}^{\rm BBN}$ is found to be at most $\simeq 0.02$. This result is consistent with $\Delta N_{\rm eff}^{\rm BBN} \lesssim 0.114$ (95% C.L.) [55]. Next, from Eq. (E2), the DM's would-be temperature today reads $\tilde{T}_{\rm DM,0} \sim \mathcal{O}(10^{-9}) \times {\rm K}$–$\mathcal{O}(10^{-8})\ {\rm K}$, which is smaller than $T_{\rm DEG} \simeq \mathcal{O}(10^{-4}) \times {\rm K}$–$\mathcal{O}(10^{-3})\ {\rm K}$. Similarly to the case of Sec. IV A, this shows that the current temperature of DM becomes low enough to accomplish the degenerate configuration when the structure formation is ignored.

V. SUB-keV FERMION DM FROM DECAY OF A SCALAR FIELD COHERENT OSCILLATION

So far we have assumed that Φ_{16} has a positive Hubble induced mass squared during the inflation. However, we assume the negative Hubble induced mass squared in this section. We consider the potential of Φ_{16},

$$V = (m_{16}^2 - c_2 H_{\rm inf}^2)|\Phi_{16}|^2 + c_{2n} \frac{1}{(n!)^2} \frac{|\Phi_{16}|^{2n}}{M_P^{2n-4}}, \tag{51}$$

where $H_{\rm inf}$ is the Hubble parameter during inflation, n is a positive integer larger than one, and c_2 and c_{2n} are positive dimensionless couplings. Then, Φ_{16} sits around the potential minimum with the amplitude $\Phi_{16,I}$ during the inflation,

$$\Phi_{16,I} \simeq \left(\frac{(n!)^2 c_2}{n c_{2n}} H_{\rm inf}^2 M_P^{2n-4}\right)^{\frac{1}{2n-2}}, \tag{52}$$

where we ignore the mass term with m_{16} by assuming $m_{16}^2 \ll c_2 H_{\rm inf}^2$. After the end of inflation, the field value of Φ_{16} is given by

$$\langle \Phi_{16} \rangle \simeq \left(\frac{(n!)^2 c_2}{n c_{2n}} H^2 M_P^{2n-4}\right)^{\frac{1}{2n-2}}, \tag{53}$$

for $n \geq 4$. Here, H denotes the Hubble expansion rate. This behavior of the scalar field is called the scaling solution [62–64]. We focus on this scaling solution with $n = 4$ as an example in the rest of this section.[21] As the Hubble expansion rate decreases and when it becomes comparable to m_{16}, the scalar field Φ_{16} starts the coherent oscillation around its origin. After that, when

[20] For ${\rm Br} \lesssim 10^{-4}$, $y_{*,\max}$ in Sec. IV B is greater than that in Sec. IV A. For a given m_{16}, with $y_{*,\max}$ being $y_{*,\max}$ given in Eq. (36), we find that $y_* \in (0.5 y_{*,\max}^{(4.1)}, 2 y_{*,\max}^{(4.1)})$ is of our interest since the range yields the desired $\lambda_{\rm FS} \in (0.3\ {\rm Mpc}, 0.5\ {\rm Mpc})$ for $m_{\rm DM} \in (200\ {\rm eV}, 400\ {\rm eV})$.

[21] We ignore the other terms with $n \neq 4$ not to affect the dynamics of Φ_{16}. The analysis for the potential with $n = 2$ or 3 will be given elsewhere.

$\Gamma(\Phi_{16} \to \psi_8 + \psi_8) \simeq H$ holds, Φ_{16} decays into the DMs.[22] This mechanism is basically the same as the one discussed in Sec. IV whereas the Φ_{16} production mechanism is different.

In the above DM production from the coherently oscillating Φ_{16}, the abundance of DM is given by

$$\left.\frac{2n_{16}}{s_{\rm SM}}\right|_{a=a_{\rm osc}} \simeq \frac{m_{16}\Phi_{16,0}^2}{\frac{2\pi^2}{45}g_{*,s}(a_{\rm osc})T_{\rm osc}^3}, \tag{54}$$

where $\Phi_{16,0}$ is the field amplitude of Eq. (53) when the oscillation of Φ_{16} starts ($H \simeq m_{16}$), i.e.,

$$\Phi_{16,0} \simeq \left(\frac{(4!)^2 c_2}{4c_8} m_{16}^2 M_P^4\right)^{\frac{1}{6}}, \tag{55}$$

$g_{*,s}$ is the effective degrees of freedom for the entropy density, and $T_{\rm osc}$ is the SM temperature at which the coherent oscillation of Φ_{16} occurs

$$T_{\rm osc} = \left(\frac{90}{\pi^2}\right)^{1/4} g_*^{-1/4}(a_{\rm osc})\sqrt{M_P m_{16}} \simeq (0.85\times 10^9)\left(\frac{g_*(a_{\rm osc})}{100}\right)^{-1/4}\left(\frac{m_{16}}{1\ \text{GeV}}\right)^{1/2}\ \text{GeV}, \tag{56}$$

where $a_{\rm osc}$ is the scale factor as the oscillation starts. Notice that we assumed that the oscillation starts at the radiation-dominated era ($T_{\rm osc} < T_R$). By attributing the whole current DM abundance to ψ_8, we demand $2n_{16}/s_{\rm SM} = Y_{\rm DM}$ at $a = a_{\rm osc}$ which yields

$$\left(\frac{g_*(a_{\rm osc})}{100}\right)^{-1/4}\left(\frac{m_{16}}{1\ \text{GeV}}\right)^{1/6}\left(\frac{m_{\rm DM}}{1\ \text{keV}}\right)\left(\frac{c_2}{c_8}\right)^{1/3} \simeq 0.6. \tag{57}$$

This result tells us that for a given c_2/c_8, there is a one to one map between $m_{\rm DM}$ and m_{16}. As an example, for $c_2/c_8 = 1, 5, 10$, we show this map in Fig. 6.

After the right amount of Φ_{16} is generated, in order to have ψ_8 as a degenerate fermion DM candidate today, we demand that

$$T_{\rm osc} > T_{\rm SM,2} \tag{58}$$

[22]Regarding the constraint from the isocurvature perturbations, the fluctuation of Φ_{16} is imprinted in the DMs in our mechanism. Thus, we assume $c_2 \gtrsim \mathcal{O}(10)$ to suppress the isocurvature perturbations (see, e.g., Ref. [65]). Note that the fluctuation of the axial component of Φ_{16} is not suppressed by this way, but this does not matter because only the fluctuation of the radial component of Φ_{16} leads to the isocurvature perturbations of the DM.

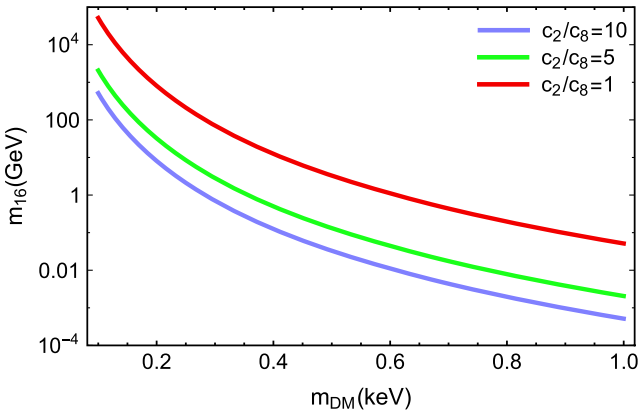

FIG. 6. The map between $m_{\rm DM}$ and m_{16} obtained by the DM relic density matching in Eq. (57).

where $T_{\rm SM,2}$ was defined in Eq. (34). This leads to

$$y_* < 2.7 \times \left(\frac{g_*(a_{\rm osc})}{100}\right)^{-1/4} \equiv y_{*,1}. \tag{59}$$

In addition, as discussed in Sec. IV A, we require

$$y_* \lesssim (10^{-6})\left(\frac{m_{\rm DM}}{1\ \text{keV}}\right)^{1/5}\left(\frac{m_{16}}{1\ \text{GeV}}\right)^{3/10} \equiv y_{*,3}, \tag{60}$$

so that the DMs do not form a thermal bath via their self-interaction through Φ_{16} exchanges after its production. Define $y_{*,\max} \equiv \min(y_{*,1}, y_{*,3})$. Now for a set of $(m_{16}, m_{\rm DM}, c_2/c_8)$ satisfying Eq. (57), $y_{*,\max}$ is determined, and by choosing a $y_* \lesssim y_{*,\max}$, $\lambda_{\rm FS}$ can be computed based on Eq. (40) and required to be 0.3 Mpc $< \lambda_{\rm FS} <$ 0.5 Mpc. For an example of $c_2/c_8 = 5$, we go through this procedure to constrain the space of the Yukawa coupling between DM and Φ_{16}, of which the result is shown in Fig. 7.

For this y_*, it turns out that Φ_{16} decay takes place before the BBN era ($a_p \simeq \mathcal{O}(10^{-15}) - \mathcal{O}(10^{-11})$) and therefore

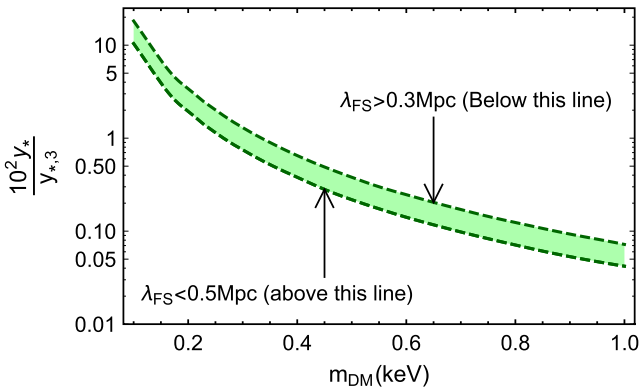

FIG. 7. For $c_2/c_8 = 5$ and $(m_{16}, m_{\rm DM})$ given in Fig. 6, requiring 0.3 Mpc $< \lambda_{\rm FS} <$ 0.5 Mpc constrains the space of the Yukawa coupling between DM and Φ_{16}.

sub-keV DM contributes to $\Delta N_{\rm eff}^{\rm BBN}$. Based on Eq. (C2), we compute $\Delta N_{\rm eff}^{\rm BBN}$ attributable to DM and find it is at most ~ 0.01 to be consistent with $\Delta N_{\rm eff}^{\rm BBN} \lesssim 0.114$ (95% C.L.) [55].

From Eq. (E2), we also estimate the DM's would-be temperature today for the case with $c_2/c_8 = 5$. The results read $\tilde{T}_{\rm DM,0} \sim \mathcal{O}(10^{-8})$–$\mathcal{O}(10^{-7})$ K, which is smaller than $T_{\rm DEG} \simeq \mathcal{O}(10^{-4})$ K–$\mathcal{O}(10^{-3})$ K. This shows that the current temperature of DM becomes low enough to accomplish the degenerate configuration when structure formation is ignored. We do not go further to discuss the cases with different ratios of c_2/c_8. If one finds $\tilde{T}_{\rm DM,0} > T_{\rm DEG}$, one may arrive at a value of c_2/c_8 which is not allowed. But we note that m_{16} and $a_{\rm FS}$ are inversely correlated in Eq. (E2).

VI. CONCLUSION

In this paper, we present a well-motivated extension of the SM which can address the core-cusp problem by providing a degenerate sub-keV fermion DM candidate. The model is characterized by $U(1)_{\rm B\text{-}L}$ gauge symmetry, and two right-handed heavy neutrinos and four new chiral fermions added to the SM gauge sector and particle contents, respectively. All the fermions in the model are charged under $U(1)_{\rm B\text{-}L}$ and assigned the corresponding $Q_{\rm B\text{-}L}$'s in a way that $U(1)_{\rm B\text{-}L}$ is rendered anomaly free. It is extremely remarkable that one of the additional fermions obtains naturally a mass of $\mathcal{O}(1)$ keV because of its large B-L charge, provided that the B-L symmetry breaking scale $\sim 10^{15}$ GeV. Thus, it was shown that the chiral fermion can serve as a sub-keV fermion DM candidate of which temperature today is low enough to form a degenerate fermion halo core for a dSphs. The DM's free-streaming length is small enough to be consistent with Lyman-α forest data. Being WDM, the DM candidate in the model is also expected to resolve other small-scale problems that the ΛCDM paradigm confronts (the missing satellite and too-big-to-fail problem). Consequently, the model can resolve the small-scale issues in cosmology as well as the smallness of the active neutrino mass and the baryon asymmetry via the thermal leptogenesis.

Concerning the DM production mechanism, we argue that fermion DM produced from the decay of a complex scalar can meet the criteria for a degenerate fermion DM. In Sec. III, we showed that nonthermal DM produced from the SM particle scattering is bound to travel too large a free-streaming length. In Sec. IV, we showed that DM produced from a series of decays (inflaton decay and Φ_{16} decay) as the final product can travel the right size of the free-streaming length $\sim\mathcal{O}(0.1)$ Mpc to be consistent with the Lyman-α forest observation. Getting into more detail, we conducted the case study depending on whether a dark thermal bath forms (Sec. IV A) or not (Sec. IV B). For both cases, $\lambda_{\rm FS}$ for a fixed $m_{\rm DM}$ are parametrized by (m_{16}, y_*). We figure out that for a set of $(m_{16}, m_{\rm DM})$, the constraint applied to a choice of y_* is more stringent for the case with the formation of a dark thermal bath (Sec. IV A) than for the other case (Sec. IV B). This fact makes it easier for the case without a dark thermal bath to produce a degenerate fermion DM consistent with the free-streaming length criterion. In Sec. V, we studied a different mechanism to produce the degenerate fermion DM via the decay of a scalar field coherent oscillation. Differing from Sec. IV where a positive Hubble induced mass is assumed during inflation, a negative Hubble induced mass during inflation is assumed in Sec. V. We studied a potential of Φ_{16} in Eq. (51) by which the Φ_{16} field is located away from the origin in the field space at the end of the inflation. For a fixed c_2/c_8, there is a one to one map between $m_{\rm DM}$ and m_{16}, which is required by DM relic density matching. Taking, for example, $c_2/c_8 = 5$, we showed how the free-streaming length criterion 0.3 Mpc $\lesssim \lambda_{\rm FS} \lesssim$ 0.5 Mpc can constrain Yukawa coupling between the mother scalar field with $\sim m_{16} \in (10^{-3}, 10^{3})$ GeV and the DM candidate. For all distinct DM production mechanisms, we also performed further consistency checks including $\Delta N_{\rm eff}^{\rm BBN}$ contributed by DM and $\tilde{T}_{\rm DM,0} < T_{\rm DEG}$. Finally, we note that the framework presented in this paper shows that even if the fermion warm DM mass is as low as the sub-keV regime, it can still travel the free-streaming length as short as $\sim\mathcal{O}(0.1)$ Mpc consistent with the Lyman-α forest observation thanks to the nontrivial dark sector structure and its cosmological history.

ACKNOWLEDGMENTS

T. T. Y. is supported in part by the China Grant for the Talent Scientific Start-Up Project and the JSPS Grant-in-Aid for Scientific Research No. 16H02176, No. 17H02878, and No. 19H05810 and by the World Premier International Research Center Initiative (WPI Initiative), MEXT, Japan. M. S. and T. T. Y. thank Kavli IPMU for their hospitality during the corona virus outbreak.

APPENDIX A: ξ DECAY

ξ is expected to decay to the SM Higgs and a lepton via the decay operator

$$\mathcal{O}_{\rm de} = \beta \frac{(\Phi_{-2}^*)^2}{M_P} \psi_{-5} \bar{N} \tag{A1}$$

where β is a dimensionless coefficient. For $V_{\rm B\text{-}L} \sim 3 \times 10^{15}$ GeV, $m_\xi \simeq 2 \times 10^9$ GeV. When the mass of the lightest right-handed neutrino is about 10^9 GeV and its mass mixing with ξ is $\mathcal{O}(1)$, ξ can immediately decay into a Higgs and a lepton via the mixing once ξ becomes nonrelativistic.

APPENDIX B: HIGGS PORTAL

The Higgs portal operator $\sim\lambda_*(H^\dagger H)|\Phi_{16}|^2$ allows for direct coupling between Φ_{16} and the SM sector at the renormalizable level. The interaction rate for the process

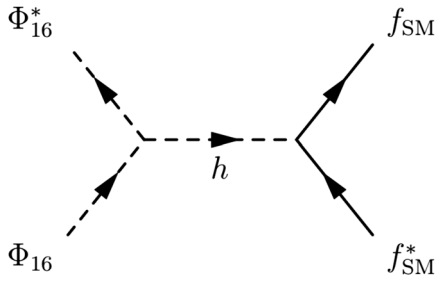

FIG. 8. For $m_{16} < \Lambda_{\rm EW}$, Φ_{16} is easily pair annihilated to the SM fermion pairs. h is the Higgs field fluctuation around the global minimum of its potential.

$H^* + H \to \Phi_{16}^* + \Phi_{16}$ owing to the Higgs portal operator, i.e., $\sim\lambda_*^2 T$, is relatively much larger than both the interaction rate for the process $f_{\rm SM}^* + f_{\rm SM} \to \Phi_{16}^* + \Phi_{16}$ via $U(1)_{\rm B\text{-}L}$ gauge boson exchange, $\sim T^5/V_{\rm B\text{-}L}^4$, and the Hubble expansion rate since reheating time, unless the Higgs portal is greatly suppressed. This tells us that produced from scattering among the SM Higgs, Φ_{16} would be easily thermalized by the SM thermal bath with significant λ_*. Once Φ_{16} joins the SM thermal bath, trivially it never decouples. For the case where Φ_{16} decays before Φ_{16} becomes nonrelativistic, ψ_8 becomes thermal WDM[23] which is out of our interest. On the contrary, if Φ_{16} becomes nonrelativistic before its decay to the DM starts, Φ_{16} would disappear prior to production of ψ_8.[24] For these reasons, for the purpose of having a sub-keV nonthermal fermion WDM, it is necessary for us to assume a highly suppressed Higgs portal operator $\sim\lambda_*(H^\dagger H)|\Phi_{16}|^2$.

APPENDIX C: $\Delta N_{\rm eff}$ CONTRIBUTED BY DM (ψ_8)

Recalling the expression for the radiation energy density

$$\rho_{\rm rad}(T \lesssim 1\ {\rm MeV}) \simeq \rho_\gamma\left(1 + \frac{7}{8}\left(\frac{4}{11}\right)^{4/3} N_{\rm eff}\right), \tag{C1}$$

we compute the extra contribution to radiation from the relativistic DM at the BBN era by

$$\Delta N_{\rm eff}^{\rm BBN} \simeq \frac{\rho_{\rm DM}}{\rho_\gamma} \times \frac{8}{7}\left(\frac{11}{4}\right)^{4/3}, \tag{C2}$$

where, based on Eq. (12), the DM energy density at the BBN time reads

$$\begin{aligned}\rho_{\rm DM}(a_{\rm BBN}) = &\sqrt{m_{\rm DM}^2 + \left(\frac{m_{16} a_{\rm FS}}{2 a_{\rm BBN}}\right)^2} \\ &\times \left[4.07 \times 10^{-4} \times \left(\frac{m_{\rm DM}}{1\ {\rm keV}}\right)^{-1}\right] \\ &\times \frac{2\pi^2}{45} g_{s,{\rm SM}}(a_{\rm BBN}) T_{\rm SM}(a_{\rm BBN})^3,\end{aligned} \tag{C3}$$

and the photon density is

$$\rho_\gamma(a_{\rm BBN}) = \frac{\pi^2}{30} \times 2 \times (1\ {\rm MeV})^4. \tag{C4}$$

APPENDIX D: MAPPING THE THERMAL WDM MASS TO A NONTHERMAL WDM

It was observed in Ref. [60] that the linear matter power spectra associated with different WDM models are very similar when the same variance of velocity and the comoving Jean scale (k_J) are assumed. The comoving Jean scale at the matter-radiation equality time is defined as [60]

$$k_J = a\sqrt{\frac{4\pi G \rho_m}{\sigma^2}}\bigg|_{a=a_{\rm eq}}, \tag{D1}$$

where ρ_m is the matter density and σ is the velocity variance of DM.

In accordance with this, it was argued in Ref. [66] that equating the warmness parameters for the thermal WDM and WDM of another type differing from the thermal one constructs the map between masses. The warmness parameter ($\sigma \equiv \tilde{\sigma} T/m$) of a WDM introduced in [66] is defined with temperature T, mass m, and the quantity

$$\tilde{\sigma} \equiv \frac{\int dq q^4 f(q)}{\int dq q^2 f(q)}, \tag{D2}$$

where $f(p)$ is the momentum space distribution function and $q \equiv p/m$ is used. To establish the map from the thermal WDM mass to another WDM candidate (χ), one can begin with

$$\sigma_\chi = \sigma_{\rm wdm} \Leftrightarrow \tilde{\sigma}_\chi \frac{T_\chi}{m_\chi} = \tilde{\sigma}_{\rm wdm} \frac{T_{\rm wdm}}{m_{\rm wdm}}, \tag{D3}$$

where σ_χ is the warmness of χ WDM and $\sigma_{\rm wdm}$ is that of the early decoupled thermal WDM. This equation tells us that

[23]The abundance of the WDM will be larger than the current dark matter abundance.

[24]If Φ_{16} is heavier than the EW symmetry breaking scale, it will be Boltzmann suppressed once $T_{\rm SM} \simeq m_{16}$ is reached. If it is lighter than the EW symmetry breaking scale, Φ_{16} is still living in the SM thermal bath by interaction with the SM fermions induced by the virtual SM Higgs. By comparing the relevant interaction rate of the diagram in Fig. 8 to the Hubble expansion rate

$$\Gamma \simeq \frac{\lambda_*^2 m_f^2}{m_h^4} T_{\rm SM}^3 \simeq \frac{T_{\rm SM}^2}{M_P} \simeq H \Rightarrow T_{\rm SM} \simeq \frac{m_h^4}{\lambda_*^2 m_f^2 M_P} \tag{B1}$$

it is realized that Φ_{16} would easily pair annihilate to SM fermions at $T_{\rm SM} \simeq m_{16}$. Here, m_f is a SM fermion mass and m_h is the physical Higgs particle mass.

once one knows T_χ, $T_{\rm wdm}$, and $\tilde{\sigma}_\chi$ at $a = a_{\rm eq}$, one can map the constraint on $m_{\rm wdm}$ to that on m_χ, knowing $\tilde{\sigma}_{\rm wdm} = 3.6$ from the Fermi-Dirac distribution. T_χ and $\tilde{\sigma}_\chi$ are closely related to the production mechanism of χ WDM. On the other hand, for the early decoupled thermal WDM, $T_{\rm wdm}$ is determined by the DM relic density. Today, a comparison of thermal WDM to the neutrino gives [67]

$$\Omega_{\rm wdm}h^2 \simeq 0.12 = \left(\frac{m_{\rm wdm}}{94\ {\rm eV}}\right)\left(\frac{T_{\rm wdm,0}}{T_{\nu,0}}\right)^3 \Leftrightarrow T_{\rm wdm,0} = \left[0.036\left(\frac{94\ {\rm eV}}{m_{\rm wdm}}\right)\right]^{1/3} T_{\gamma,0}., \tag{D4}$$

where $T_{\nu,0} = (4/11)^{1/3}T_{\gamma,0}$ is today's neutrino temperature.

APPENDIX E: WOULD-BE TEMPERATURE OF DM CANDIDATE

The necessary condition that the fermion DM candidate should satisfy to form a cored halo profile within a dSphs is that its would-be temperature today ($\tilde{T}_{\rm DM,0}$) in the absence of structure formation should be smaller than a degeneracy temperature for the dSphs ($T_{\rm DEG}$) [28]. From the property that DM's momentum scales as $\sim a^{-1}$ and the temperature of DM that can be defined via $E_k \sim kT$, we can infer that the DM's temperature scales as $\sim a^{-1}$ for the relativistic state and $\sim a^{-2}$ for the nonrelativistic state.

For the case where the fermion DM candidate is produced from a nonrelativistic scalar decay and free stream since then, the scale factor ($a_{\rm NR}$) at which DM becomes nonrelativistic is given by

$$a_{\rm NR} \simeq \frac{m_S a_{\rm FS}}{2m_{\rm DM}}, \tag{E1}$$

where m_S is the mother scalar's mass and $a_{\rm FS}$ is the scale factor at which DM starts free streaming. Therefore, starting with $p_{\rm DM}(a_{\rm FS}) \simeq m_S/2$, the would-be temperature for DM today is computed by

$$\tilde{T}_{\rm DM,0} \simeq \frac{m_S a_{\rm FS}}{2a_{\rm NR}} \times \left(\frac{a_{\rm NR}}{a_0}\right)^2 = m_{\rm DM}\left(\frac{m_S a_{\rm FS}}{2m_{\rm DM}}\right)^2, \tag{E2}$$

where Eq. (E1) is used for the second equality. The degeneracy temperature for a dSphs used for checking is roughly $T_{\rm DEG} \simeq \mathcal{O}(10^{-4})$ K–$\mathcal{O}(10^{-3})$ K [28].

[1] J. F. Navarro, C. S. Frenk, and S. D. M. White, A universal density profile from hierarchical clustering, Astrophys. J. **490**, 493 (1997).
[2] T. Fukushige and J. Makino, On the origin of cusps in dark matter halos, Astrophys. J. **477**, L9 (1997).
[3] T. Ishiyama, J. Makino, S. Portegies Zwart, D. Groen, K. Nitadori, S. Rieder, C. d. Laat, S. McMillan, K. Hiraki, and S. Harfst, The cosmogrid simulation: Statistical properties of small dark matter halos, Astrophys. J. **767**, 146 (2013).
[4] A. Borriello and P. Salucci, The dark matter distribution in disk galaxies, Mon. Not. R. Astron. Soc. **323**, 285 (2001).
[5] G. Gilmore, M. I. Wilkinson, R. F. G. Wyse, J. T. Kleyna, A. Koch, N. W. Evans, and E. K. Grebel, The observed properties of dark matter on small spatial scales, Astrophys. J. **663**, 948 (2007).
[6] S.-H. Oh, W. J. G. d. Blok, F. Walter, E. Brinks, and R. C. Kennicutt, Jr., Highresolution dark matter density profiles of things dwarf galaxies: Correcting for non-circular motions, Astron. J. **136**, 2761 (2008).
[7] W. J. G. de Blok, The core-cusp problem, Adv. Astron. **2010**, 789293 (2010).
[8] M. G. Walker and J. Penarrubia, A method for measuring (slopes of) the mass profiles of dwarf spheroidal galaxies, Astrophys. J. **742**, 20 (2011).
[9] B. Moore, S. Ghigna, F. Governato, G. Lake, T. R. Quinn, J. Stadel, and P. Tozzi, Dark matter substructure within galactic halos, Astrophys. J. **524**, L19 (1999).
[10] S. Y. Kim, A. H. G. Peter, and J. R. Hargis, Missing Satellites Problem: Completeness Corrections to the Number of Satellite Galaxies in the Milky Way are Consistent with Cold Dark Matter Predictions, Phys. Rev. Lett. **121**, 211302 (2018).
[11] M. Boylan-Kolchin, J. S. Bullock, and M. Kaplinghat, Too big to fail? The puzzling darkness of massive milky way subhaloes, Mon. Not. R. Astron. Soc. Lett. **415**, L40 (2011).
[12] B. Moore, T. R. Quinn, F. Governato, J. Stadel, and G. Lake, Cold collapse and the core catastrophe, Mon. Not. R. Astron. Soc. **310**, 1147 (1999).
[13] P. Bode, J. P. Ostriker, and N. Turok, Halo formation in warm dark matter models, Astrophys. J. **556**, 93 (2001).
[14] P. Colin, V. Avila-Reese, and O. Valenzuela, Substructure and halo density profiles in a warm dark matter cosmology, Astrophys. J. **542**, 622 (2000).
[15] V. Avila-Reese, P. Colin, O. Valenzuela, E. D'Onghia, and C. Firmani, Formation and structure of halos in a warm dark matter cosmology, Astrophys. J. **559**, 516 (2001).
[16] J. Zavala, Y. P. Jing, A. Faltenbacher, G. Yepes, Y. Hoffman, S. Gottlober, and B. Catinella, The velocity function in the local environment from LCDM and LWDM constrained simulations, Astrophys. J. **700**, 1779 (2009).
[17] A. V. Tikhonov, S. Gottloeber, G. Yepes, and Y. Hoffman, The sizes of mini-voids in the local universe: An argument in favor of a warm dark matter model?, Mon. Not. R. Astron. Soc. **399**, 1611 (2009).

[18] M. R. Lovell, V. Eke, C. S. Frenk, L. Gao, A. Jenkins, T. Theuns, J. Wang, D. M. White, A. Boyarsky, and O. Ruchayskiy, The haloes of bright satellite galaxies in a warm dark matter universe, Mon. Not. R. Astron. Soc. **420**, 2318 (2012).
[19] P. Colin, O. Valenzuela, and V. Avila-Reese, On the structure of dark matter halos at the damping scale of the power spectrum with and without Relict velocities, Astrophys. J. **673**, 203 (2008).
[20] A. V. Maccio, S. Paduroiu, D. Anderhalden, A. Schneider, and B. Moore, Cores in warm dark matter haloes: A Catch 22 problem, Mon. Not. R. Astron. Soc. **424**, 1105 (2012).
[21] C. Destri, H. J. d. Vega, and N. G. Sanchez, Fermionic warm dark matter produces galaxy cores in the observed scales because of quantum mechanics, New Astron. **22**, 39 (2013).
[22] S. U. Ji and S. J. Sin, Late time phase transition and the galactic halo as a bose liquid: 2. The effect of visible matter, Phys. Rev. D **50**, 3655 (1994).
[23] W. Hu, R. Barkana, and A. Gruzinov, Cold and Fuzzy Dark Matter, Phys. Rev. Lett. **85**, 1158 (2000).
[24] L. Hui, J. P. Ostriker, S. Tremaine, and E. Witten, Ultralight scalars as cosmological dark matter, Phys. Rev. D **95**, 043541 (2017).
[25] M. Rocha, A. H. G. Peter, J. S. Bullock, M. Kaplinghat, S. Garrison-Kimmel, J. Onorbe, and L. A. Moustakas, Cosmological simulations with self-interacting dark matter I: Constant density cores and substructure, Mon. Not. R. Astron. Soc. **430**, 81 (2013).
[26] A. H. G. Peter, M. Rocha, J. S. Bullock, and M. Kaplinghat, Cosmological simulations with self-interacting dark matter II: Halo shapes vs. observations, Mon. Not. R. Astron. Soc. **430**, 105 (2013).
[27] D. N. Spergel and P. J. Steinhardt, Observational Evidence for Selfinteracting Cold Dark Matter, Phys. Rev. Lett. **84**, 3760 (2000).
[28] V. Domcke and A. Urbano, Dwarf spheroidal galaxies as degenerate gas of free fermions, J. Cosmol. Astropart. Phys. 01 (2015) 002.
[29] L. Randall, J. Scholtz, and J. Unwin, Cores in dwarf galaxies from Fermi repulsion, Mon. Not. R. Astron. Soc. **467**, 1515 (2017).
[30] D. Savchenko and A. Rudakovskyi, New mass bound on fermionic dark matter from a combined analysis of classical dSphs, Mon. Not. R. Astron. Soc. **487**, 5711 (2019).
[31] C. Di Paolo, F. Nesti, and F. L. Villante, Phase space mass bound for fermionic dark matter from dwarf spheroidal galaxies, Mon. Not. R. Astron. Soc. **475**, 5385 (2018).
[32] S. M. K. Alam, J. S. Bullock, and D. H. Weinberg, Dark matter properties and halo central densities, Astrophys. J. **572**, 34 (2002).
[33] S. Shao, L. Gao, T. Theuns, and C. S. Frenk, The phase-space density of fermionic dark matter haloes, Mon. Not. R. Astron. Soc. **430**, 2346 (2013).
[34] S. Alexander and S. Cormack, Gravitationally bound BCS state as dark matter, J. Cosmol. Astropart. Phys. 04 (2017) 005.
[35] B. G. Giraud and R. Peschanski, Profile of a galactic spherical cloud of self-gravitating Fermions, Phys. Scr. **94**, 085003 (2019).
[36] K. Pal, L. V. Sales, and J. Wudka, Ultralight Thomas-Fermi dark matter, Phys. Rev. D **100**, 083007 (2019).
[37] M. Viel, G. D. Becker, J. S. Bolton, and M. G. Haehnelt, Warm dark matter as a solution to the small scale crisis: New constraints from high redshift Lyman-α forest data, Phys. Rev. D **88**, 043502 (2013).
[38] J. Baur, N. Palanque-Delabrouille, C. Yèche, C. Magneville, and M. Viel, Lymanalpha forests cool warm dark matter, J. Cosmol. Astropart. Phys. 08 (2016) 012.
[39] V. Iršič *et al.*, New constraints on the free-streaming of warm dark matter from intermediate and small scale Lyman-α forest data, Phys. Rev. D **96**, 023522 (2017).
[40] F. Borzumati, T. Bringmann, and P. Ullio, Dark matter from late decays and the small-scale structure problems, Phys. Rev. D **77**, 063514 (2008).
[41] J. A. R. Cembranos, J. L. Feng, A. Rajaraman, and F. Takayama, SuperWIMP Solutions to Small Scale Structure Problems, Phys. Rev. Lett. **95**, 181301 (2005).
[42] T. Yanagida, Horizontal gauge symmetry, and masses of neutrinos, Conf. Proc. C **7902131**, 95 (1979).
[43] M. Gell-Mann, P. Ramond, and R. Slansky, Complex spinors and unified theories, Conf. Proc. C **790927**, 315 (1979).
[44] P. Minkowski, $\mu \to e\gamma$ at a rate of one out of 10^9 muon decays? Phys. Lett. **67B**, 421 (1977).
[45] M. Fukugita and T. Yanagida, Baryogenesis without grand unification, Phys. Lett. B **174**, 45 (1986).
[46] K. Nakayama, F. Takahashi, and T. T. Yanagida, Number-theory dark matter, Phys. Lett. B **699**, 360 (2011).
[47] K. Nakayama, F. Takahashi, and T. T. Yanagida, Revisiting the number-theory dark matter scenario and the weak gravity conjecture, Phys. Lett. B **790**, 218 (2019).
[48] G. Choi, M. Suzuki, and T. T. Yanagida, Degenerate sub-keV Fermion dark matter from a solution to the Hubble Tension, Phys. Rev. D **101**, 075031 (2020).
[49] P. H. Frampton, S. L. Glashow, and T. Yanagida, Cosmological sign of neutrino *CP* violation, Phys. Lett. B **548**, 119 (2002).
[50] A. d. Gouvea, See-saw energy scale, and the LSND anomaly, Phys. Rev. D **72**, 033005 (2005).
[51] T. Asaka, S. Blanchet, and M. Shaposhnikov, The nuMSM, dark matter and neutrino masses, Phys. Lett. B **631**, 151 (2005).
[52] A. Kusenko, F. Takahashi, and T. T. Yanagida, Dark matter from split Seesaw, Phys. Lett. B **693**, 144 (2010).
[53] S. Khalil and O. Seto, Sterile neutrino dark matter in B-L extension of the standard model and galactic 511-keV line, J. Cosmol. Astropart. Phys. 10 (2008) 024.
[54] G. Choi, M. Suzuki, and T. T. Yanagida, XENON1T anomaly and its implication for decaying warm dark matter, arXiv:2006.12348.
[55] B. D. Fields, K. A. Olive, T.-H. Yeh, and C. Young, Big-Bang nucleosynthesis after Planck, J. Cosmol. Astropart. Phys. 03 (2020) 010.
[56] A. Garzilli, O. Ruchayskiy, A. Magalich, and A. Boyarsky, How warm is too warm? Towards robust Lyman-α forest bounds on warm dark matter, arXiv:1912.09397.
[57] M. Kaplinghat, Dark matter from early decays, Phys. Rev. D **72**, 063510 (2005).

[58] L. E. Strigari, M. Kaplinghat, and J. S. Bullock, Dark matter halos with cores from hierarchical structure formation, Phys. Rev. D **75**, 061303 (2007).
[59] S. Aoyama, K. Ichiki, D. Nitta, and N. Sugiyama, Formulation and constraints on decaying dark matter with finite mass daughter particles, J. Cosmol. Astropart. Phys. 09 (2011) 025.
[60] A. Kamada, N. Yoshida, K. Kohri, and T. Takahashi, Structure of dark matter halos in warm dark matter models and in models with long-lived charged massive particles, J. Cosmol. Astropart. Phys. 03 (2013) 008.
[61] A. Merle, V. Niro, and D. Schmidt, New production mechanism for keV sterile neutrino dark matter by decays of frozen-in scalars, J. Cosmol. Astropart. Phys. 03 (2014) 028.
[62] A. R. Liddle and R. J. Scherrer, A classification of scalar field potentials with cosmological scaling solutions, Phys. Rev. D **59**, 023509 (1999).
[63] K. Harigaya, M. Ibe, M. Kawasaki, and T. T. Yanagida, Dynamics of Peccei-Quinn breaking field after inflation and axion isocurvature perturbations, J. Cosmol. Astropart. Phys. 11 (2015) 003.
[64] M. Ibe, S. Kobayashi, M. Suzuki, and T. T. Yanagida, Dynamical solution to the axion domain wall problem, Phys. Rev. D **101**, 035029 (2020).
[65] A. Riotto, Inflation, and the theory of cosmological perturbations, ICTP Lect. Notes Ser. **14**, 317 (2003).
[66] A. Kamada and K. Yanagi, Constraining FIMP from the structure formation of the Universe: Analytic mapping from m_{wdm}, J. Cosmol. Astropart. Phys. 11 (2019) 029.
[67] M. Viel, J. Lesgourgues, M. G. Haehnelt, S. Matarrese, and A. Riotto, Constraining warm dark matter candidates including sterile neutrinos and light gravitinos with WMAP and the Lyman-alpha forest, Phys. Rev. D **71**, 063534 (2005).